Hindawi
Geofluids
Volume 2023, Article ID 1693773, 11 pages
https://doi.org/10.1155/2023/1693773

*Research Article*

# Study on the Coupling Law between Pore-Scale Fluid Flow Capacity and Pore-Throat Configuration in Tight Sandstone Reservoirs

**Jie Gao**,[1] **Hu Wei**,[2] **Ran Zhou**,[3] **Qiang Ren**,[4] **Tao Tian**,[5] **Bo Ning**,[6] **Xiaojun Ding**,[7] **and Zhifeng Zhang**[8]

[1]*School of Civil Engineering & Geodesy, Shaanxi College of Communication Technology, Xi'an 710018, China*
[2]*Research Institute of Shaanxi Yanchang Petroleum (Group) Co., Ltd., Xi'an, Shaanxi 710075, China*
[3]*Drilling and Production Technology Research Institute, CNPC Chuanqing Drilling Engineering Company Limited, Xi'an Shaanxi 710021, China*
[4]*School of Geology Engineering and Geomatics, Chang'an University, Xi'an 710054, China*
[5]*Key Laboratory of Coal Resources Exploration and Comprehensive Utilization, Ministry of Natural Resources, Xi'an 710021, China*
[6]*PetroChina Research Institute of Petroleum Exploration & Development, Beijing 100083, China*
[7]*Research Institute of Exploration and Development, PetroChina Qinghai Oilfield Company, Dunhuang 736202, China*
[8]*National Engineering Laboratory for Exploration and Development of Low Permeability Oil and Gas Fields, Xi'an 710018, China*

Correspondence should be addressed to Jie Gao; 28372396@qq.com

Received 27 August 2022; Revised 28 December 2022; Accepted 18 March 2023; Published 11 April 2023

Academic Editor: Mohammed Fattah



As for the tight sandstones, pore-scale fluid flow ability is one of the most fundamental parameters that determine potential development capacity when compared to conventional reservoirs due to relatively tiny spaces. The determination of pore-throat structures and their impact on fluid flow behavior could improve the forecast ability for development. Therefore, the main purpose of this paper is to study the effects of differences in microscopic pore structures on moveable fluid saturation in tight sandstone reservoirs. Casting thin sections (CTS), scanning electron microscope (SEM), constant-rate mercury injection (CRMI), nuclear magnetic resonance (NMR), etc. are used as experimental methods to qualitatively describe the differences in accumulation space types and to quantitatively compare and analyze the differences in microscopic pore structures between reservoirs for Chang 6 formation in the Jiyuan and Heshui areas. The different characteristic parameters are chosen to analyze their correlations with moveable fluid saturation. Thus, as a result, due to good correlations with moveable fluid saturation, parameters such as throat radius, pore-throat radius ratio, and pore-throat amount allocation ratio are chosen to characterize the differences in microscopic pore structures between reservoirs in those areas. Differences in throat radius, pore-throat radius ratio, and a pore-throat amount allocation ratio of microscopic pore structure of Chang 6 members in these two areas have led to differences in moveable fluid saturation to some extent. This research provided the evidence about the coupling law between pore-scale fluid flow capacity and pore-throat configuration in tight sandstone reservoirs, and the results can provide theoretical guidance for field development of oil and gas fields.

## 1. Introduction

Tight sandstone reservoirs are one of the most fundamental reservoirs in China [1]. Compared to traditional reservoirs, tight reservoirs have tiny pores and complex networks, making the fluid flow ability different from the former one, and the Darcy law is not suitable for these conditions [2]. Therefore, it is vital to investigate their pore networks and fluid flow behavior with proper methods. The NMR method has been widely used in the pore networks and fluid flow ability evaluation in tight sandstone reservoirs [3]. Characteristics relating to the physical properties of a reservoir, such as a

pore fluid characteristic of a rock, effective porosity, moveable fluid, irreducible water volume, and pore structure, can all be directly obtained by analyzing the variation characteristics of the hydrogen atom of the pore fluid in an NMR experiment [4–6]. Affected by cementation and diagenesis, the pore structure characteristic in tight sandstone reservoirs is complex [7, 8]. Thus, the fluid flow characteristic in tight sandstone reservoirs is different from that in the conventional reservoir.

The microscopic pore structure of tight reservoirs and moveable fluid capacity are significant parameters in petroleum development [9]. With the improvement of technical methods, conventional mercury injection (CMI) and oil-water relative permeability (ORP) experiments are not able to meet the accuracy level where microscopic pore structures in tight sandstone reservoirs are described [6, 10]. The appearance of CRMI has made it possible to measure the pore and throat amount and has overcome the shortcomings of CMI [11–13]. However, what is worth noting is that due to the variety of attenuation factors, it is more challenging to determine moveable fluid parameters of tight sandstone cores using NMR than to determine that of conventional cores [10]. Thus, through parametric analysis of moveable fluid characteristics, the accuracy of quantitating evaluation of tight sandstone reservoir has been significantly improved.

In this research, Chang 6 members in the Jiyuan and Heshui areas of the Ordos basin are chosen as the study object (Figure 1). The reason why we chose those two areas is based on data abundance and the sedimentary criterion [14]. They are both in the west of the Ordos basin, stretching across two secondary tectonic units of the Yishaan Slope and the Tianhuan Depression. From the analysis of sedimentary characteristics of the two areas, it is found that the Jiyuan area mainly developed delta front subfacies with its sediment source coming mostly from the northeast and northwest, while the Heshui area is mainly delta front and deep-half deep lake subfacies, and its sediment source mainly came from the southwest [14]. The difference in sediment environment results in the difference in the microscopic pore structure of the two reservoirs to some extent.

## 2. Methods

In this paper, the differences in physical properties, mineral components, and microscopic pore structures of the two reservoir rocks will be analyzed, and their effects on moveable fluid will be explained. This paper tried to conclude the microscopic geological behaviors in the Ordos basin and provide a clue about the fluid flow capacity and their impact factors. Next, we introduce the procedures and instrument properties in this research.

*2.1. Physical Property Feature.* Helium porosity and nitrogen permeability were tested by Ultrapore-300 and PDP-200, respectively. The former one used helium as the media, with 200 psi test pressure, room temperature, 220 V voltage, and 50 Hz rated frequency. The latter one used nitrogen as the media, with the same temperature, voltage, and rated frequency as the former one.

*2.2. Casting Thin Section Analysis (CTS).* The rocks were cut, drilled, and polished to meet the thin section requirement: 2 cm long, 2 cm width, and 0.03 cm thick. We used the Olympus microscopy as the inspector, and NDN-100 particle sizing system was been used to measure the grain size distributions. The mineral contents were determined by the image analysis function acquired by the system.

*2.3. Scanning Electron Microscopy (SEM).* The ZEISS Supra 25 scanning electron microscopy could reflect the clay minerals distributions and has been applied in this research. The samples were first polished, covered by carbon, and then set in the cabin. We set the accelerating voltage as 20 kV and EDT inspector.

*2.4. Rate-Controlled Mercury Intrusion (CRMI).* The YRD-Hg 1000 rate-controlled mercury intrusion instrument was applied by us. The maximum intrusion pressure was set at 6.2 MPa, and the intrusion flux was 0.0005 mL/min. The inlet pressure was inspected instantly to determine the pores and throats.

*2.5. Nuclear Magnetic Resonance (NMR).* The Niumag Portable Nuclear Magnetic Resonance was the apparatus. We selected 2 MHz as the field frequency to meet the requirement that tight sandstones have tiny pores and throats. $T_2$ relaxation time was measured to evaluate the pore network distributions.

## 3. Results

*3.1. Physical Property Feature.* Although Chang 6 members in these two areas both belong to tight sandstone reservoirs, their physical properties regarding moveable fluid are significantly different: the average porosity of Chang 6 members in the Jiyuan area is 9.39%, and the average permeability is $0.43 \times 10^{-3}$ $\mu m^2$, while average porosity of Chang 6 member in the Heshui area is 9.20% with $0.15 \times 10^{-3}$ $\mu m^2$ of its permeability. These areas are close in porosity, while their permeability is proportional by a factor of two.

*3.2. Petrologic Characteristics.* According to the industry standard, SY/T 5368-2000 [15], classification of reservoir sandstones, the sandstone type of Chang 6 member in the Jiyuan area is arkose, while in the Heshui area, it is rock fragments-feldspar (Figure 2). In the Jiyuan area, the absolute content range of feldspar is 10%-71% with an average of 38%; the absolute content range of quartz is 13%-70% with an average of 31.2%; and the absolute content range of rock fragments is 0.0-33.4% with an average of 8.9%, among which metamorphic and igneous rock fragments are dominant constitutes. In the Heshui area, the absolute content range of feldspar is 7.8%-55% with an average of 22%; the absolute content range of quartz is 15.6%-84% with an average of 41.3%; and the absolute content range of rock fragments is 4.0%-36.2% with an average of 16.8%, among which metamorphic and sedimentary rock fragments are dominant constitutes (Figure 3). The petrologic characteristic differences between these two areas are mainly reflected in their absolute contents of feldspar and quartz.

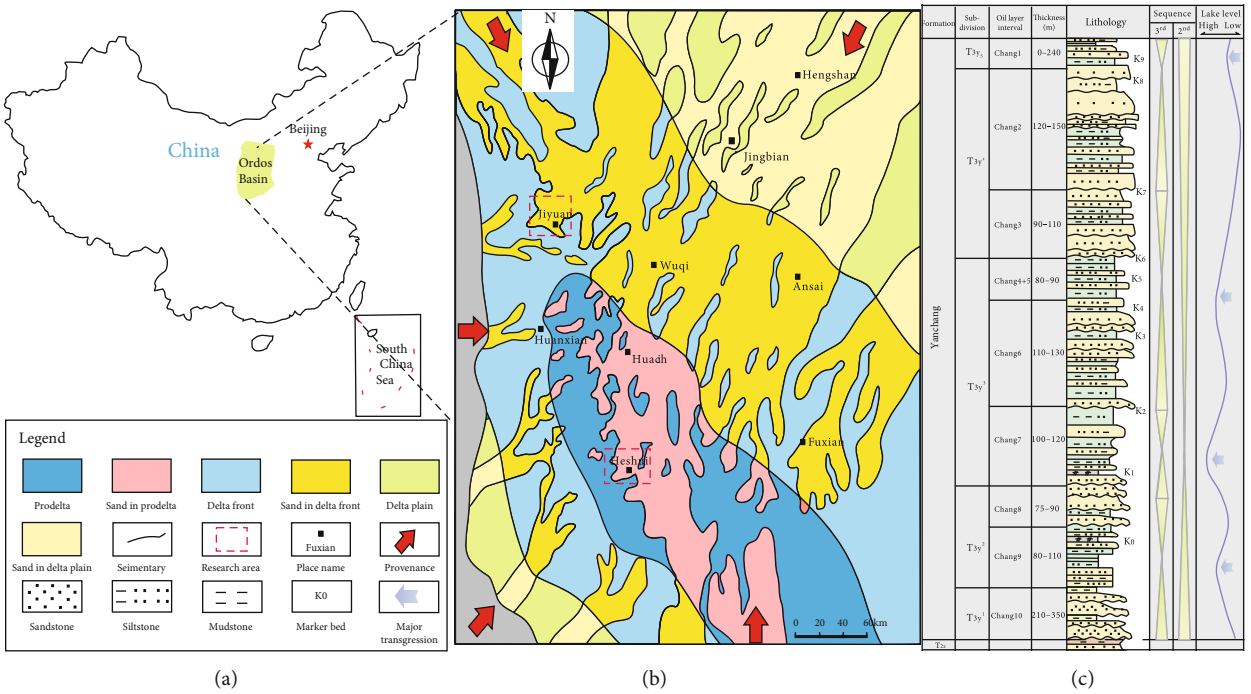


Figure 1: Geographic location and depositional setting in the research zone (modified from [14]).

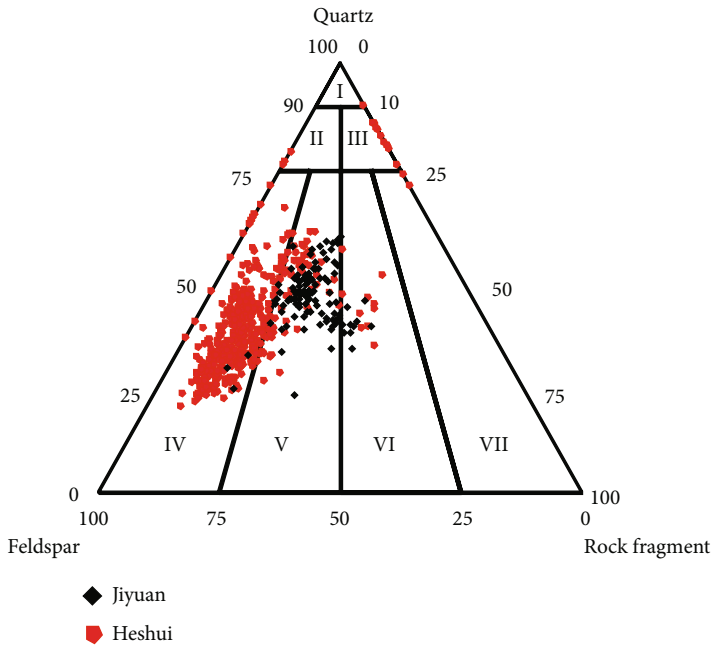


Figure 2: Characteristics and types of sandstones in the research area.

According to the grain-size analysis and CTS identification results, it is found that, in the Jiyuan area, grain sizes mainly range between 0.06 and 0.25 mm with fine-very fine sandstones taking the dominant, and few medium-grained sandstones appear. The sorting of sandstone detrital grains is good in this area, but its psephicity is poor, and grains are mainly subangular. Cementation types in this area are mainly pore and enlarged-pore cementation, while in the Heshui area, grain sizes mainly range between 0.05 and 0.24 mm with fine-very fine sandstones appearing the most. Sandstone detrital grains in this area are medially sorted with poor psephicity and subangular. Cementation types are the same as that in the Jiyuan area, mainly pore and enlarged-poor cementation (Figure 4).

The results of X-ray diffraction analysis show that (39 samples in total, among which 21 are from the Jiyuan area and 18 from the Heshui area) interstitial materials in sandstones of Chang 6 member of both areas are mainly

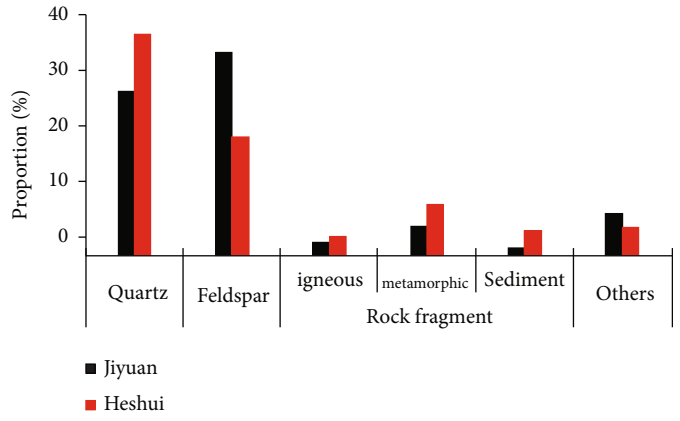


Figure 3: Fragment compositions in the research areas.

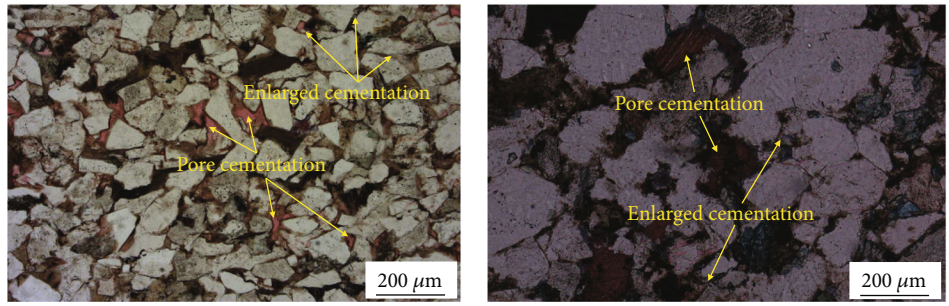


(a) (b)

Figure 4: Characteristics of psephicity and cementation types in the (a) Jiyuan and (b) Heshui areas.

kaolinite, illite, chlorite, ferrocalcite, ankerite, calcite, and silicate, etc. Figure 5 shows that the difference in interstitial materials of the two areas is mainly reflected from the differences in the absolute contents of kaolinite, illite, chlorite, calcite, and matrix.

*3.3. Microscopic Pore Structures by Microscopic Images.* The pore structure of the rock is the most direct microscopic property reflecting the quality of a reservoir, and microscopic pore structure affects the occurrence and permeability of underground fluid [16–18]. Currently, there are various ways of studying pore structure in the reservoir [19–21], and in this paper, microscopic observation combined with mercury injection is used.

Through the analysis of the extensive CTS from Chang 6 members of both Jiyuan and Heshui areas, seldom differences have been found in pore structures of the two areas, of which the main types are residual intergranular pore, feldspar dissolution pore, detritus dissolution pore, and intracrystalline pore, with a few microscopic fractures that appear (Figure 6).

From the analysis of CTS of the clastic rocks (63 samples in total, among which 34 are from the Jiyuan area and 29 from the Heshui area) and counting of fractions of every pore structure type in the total facial porosity in the Jiyuan and the Heshui areas, it is found that in the Jiyuan area, residual intergranular pores, feldspar dissolution pores, rock fragment dissolution pores, intracrystalline pores, and microscopic fracture account for 32.53%, 50.38%, 13.05%, 2.98%, and 1.06%, respectively, while in the Heshui area, the aforementioned pore-throat-cracks account for 29.57%, 40.43%, 18.06%, 10.97%, and 0.97%, respectively (Figure 7). It is concluded from the comparison of pore structures in the two areas that the difference is mainly reflected by a higher residual intergranular pore fraction in the Jiyuan area than that in the Heshui area, and the total dissolution pores developed better in the former area, among which feldspar dissolution pore developed the most.

*3.4. Microscopic Pore Structures by CRMI.* For further analysis of reservoir pore-throat sizes and their spatial arrangement in the two areas, CRMI experiment has been introduced here. Compared to CMI, the assumed model of the CRMI experiment is more applicable to tight sandstone reservoirs whose structure characteristics are small pore-fine throat or fine pore-microscopic throat. The model of CRMI is much closer to the real pore structure in a reservoir, and the shortcomings of CMI have been overcome by being able to directly measure the size and amount of pore and throat [22, 23].

CRMI experience has been applied to 7 samples from the Jiyuan area and 6 samples from the Heshui area, respectively. Table S1 shows what has been sorted out from the experiment. The results show that the values of effective pore volume and effective throat volume of the two areas are close, indicating that the volume of their accumulation

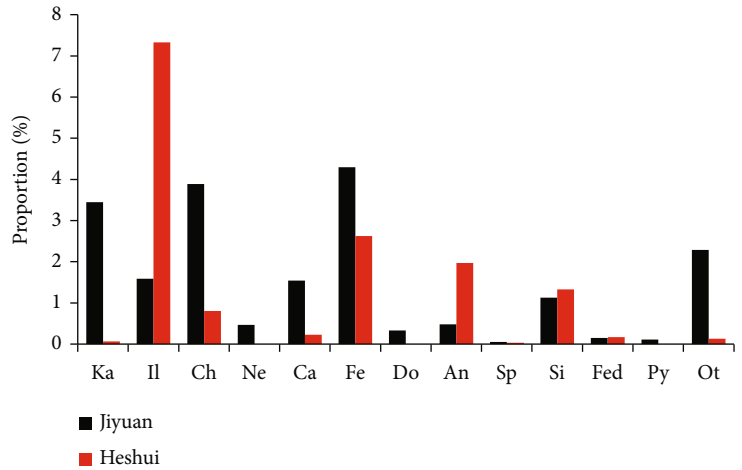


Figure 5: Interstitial materials in the research areas. Ka: kaolinite; Il: illite; Ch: chlorite; Ne: ne; Ca: carbonate; Fe: ferrocalcite; Do: dolomite; An: ankerite; Sp: specity; Si: silica; Fed: ferrodolomite; Py: pyrite; Ot: others.

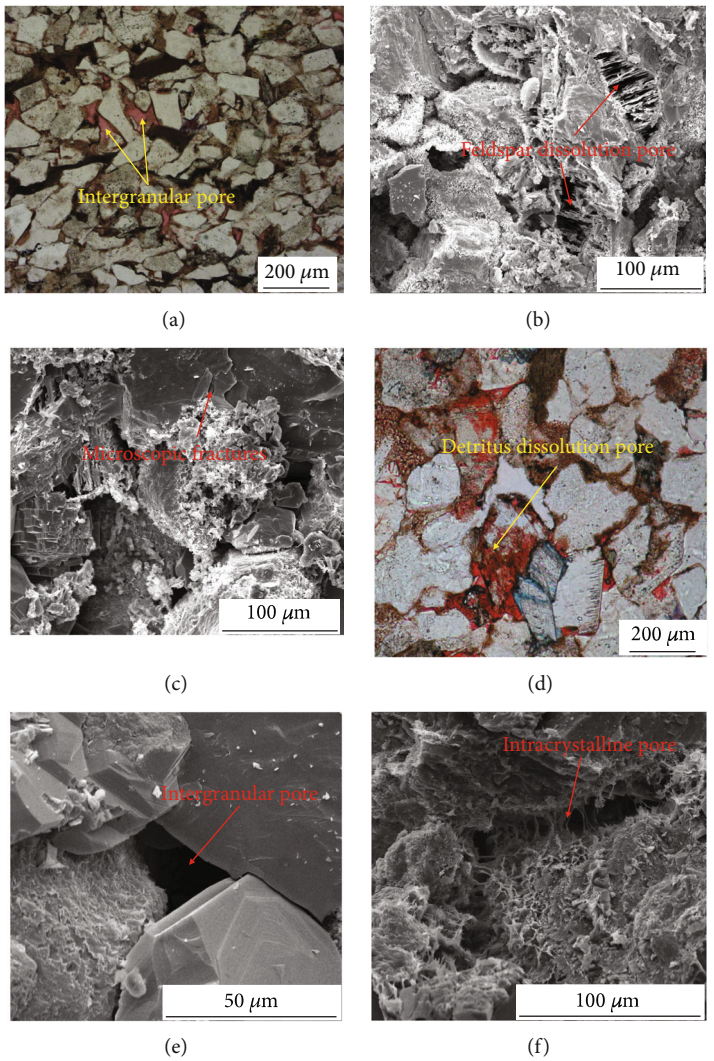


Figure 6: Photographs of CTS and SEM in the (a) Jiyuan and (b) Heshui areas.

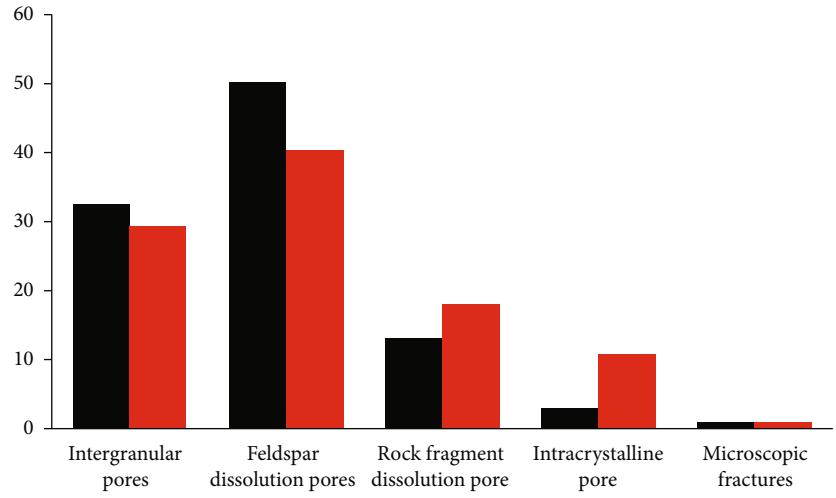


Figure 7: Fractions of different pore types in the research area.

spaces is close. In the Heshui area, pore and throat mercury injection saturation is 23.20% and 21.90%, respectively, while that in the Jiyuan area is 29.47% and 24.93%, respectively. Between those two areas, there is a great difference in mercury injection saturation resulting from the sizes and spatial arrangement of pores and throats. In the Heshui area, the amount of throat is 1992.83 per cubic centimeter, and the amount of pore is 1506.00 per cubic centimeter, while in the Jiyuan area, the amount of throat is 2246.86 per cubic centimeter, and the pore is 1431.29 per cubic centimeter. The difference in the amount of throat mainly reflects the difference in the total amount of pore and throat in the two areas. Thus, the pore-throat amount allocation ratio per unit volume, $N_R$, has been introduced here to compare the difference in pore and throat allocation between the two areas:

$$N_R = \frac{N_T}{N_P}, \tag{1}$$

where $N_P$ is the amount of pore per unit volume (/cm$^3$) and $N_T$ is the amount of throat per unit volume (/cm$^3$).

In the Jiyuan area, the average $N_R$ is 1.57 meaning that in average 1 pore corresponds to 1.57 throat, while in the Heshui area, the average $N_R$ is 1.32 meaning that 1 pore only corresponds to 1.32 throat. From the pore-throat amount allocation ratio, it is found that in the Jiyuan area, every pore connects with more amount of throat than that in the Heshui area indicating that pore connectivity in the former one is better than that in the latter one since throat is the main channel for the fluid to permeate in the reservoir.

The average pore radius of the two areas is close. In the Jiyuan area, the average pore radius is 128.48 $\mu$m, and in the Heshui area, it is 133.20 $\mu$m. However, there is a great difference in their average throat radius, and the Jiyuan area has developed more wide throat. The average throat radius in the Jiyuan area is 0.61 $\mu$m, while in the Heshui area, the average throat radius is 0.35 $\mu$m. More amount of big throat in the Jiyuan area makes this area better in the total microscopic pore structure and higher in the total mercury injection saturation.

Pore-throat radius ratio reflects the difference in the sizes of pore and throat and the heterogeneity of microscopic pore structure in the reservoir. The higher the radius ratio, the stronger the heterogeneity of the reservoir. In the Jiyuan area, the radius ratio is 209.5, while in the Heshui area, the ratio is as high as 378.94. This means that the heterogeneity of the microscopic pore-throat structure in the Heshui area is higher than that in the Jiyuan area.

*3.5. Movable Fluid Properties.* Based on the study of differences in the microscopic pore structure of Chang 6 members between the two areas, samples have been selected (13 samples in total among which 7 are from the Jiyuan area and 6 from the Heshui area) to apply on NMR. In this research, the $T_2$ cut-off point is selected to be 13.895 ms. The difference in moveable fluid saturation of these two areas is up to 7.71%, and the average moveable fluid saturation in the Jiyuan area is 43.02%, while in the Heshui area, it is only 35.31%. In the experiment, two types of NMR $T_2$ curve of Chang 6 members in both the two areas have been observed: double peak and single peak (Figure 8).

In the Jiyuan area, shapes of $T_2$ curves are mostly double peak, and the shape of secondary peaks is easily observed. Most of the main peaks of the 7 samples in the Jiyuan area locate at the fluid immobile region except that the main peak of sample H192 locates at the mobile region, while in the Heshui area, $T_2$ curves show a single-peak shape, and their main peaks and secondary peaks do not show a huge difference. All the main peaks of $T_2$ curves of those 6 samples in the Heshui area locate at the immobile region. According to experimental results, the average moveable fluid saturation of the Jiyuan area is 43.02%, and all the 7 samples from this area are type III which is a moderate reservoir according to the NMR moveable fluid evaluation standard, while in the Heshui area, the average moveable fluid saturation is only 35.31%, and the irreducible water saturation is relatively high. Three samples out of 6 from the Heshui area are type

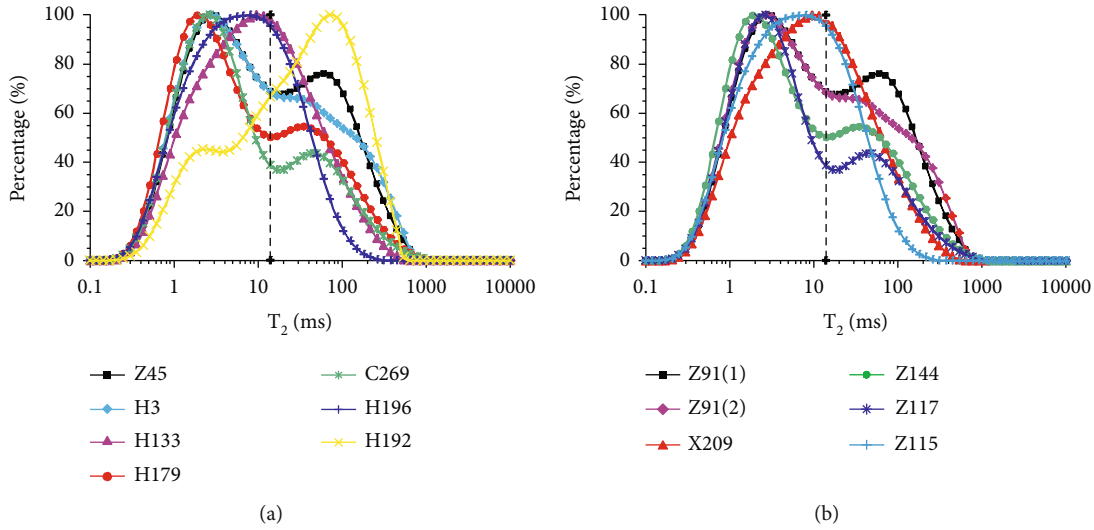


FIGURE 8: $T_2$ curves of the (a) Jiyuan and (b) Heshui areas.

III, the moderate reservoir, and the rest of the 3 samples are type IV, which is a poor reservoir (Table S2).

## 4. Discussion

*4.1. Effects on Moveable Fluid Parameters of Physical Properties.* The correlation between physical properties and movable fluid parameters in the two regions is not strong, indicating that physical properties are not the main controlling factor of movable fluid properties in the two regions as a whole (Figure 9). Generally speaking, the higher the porosity or permeability, the greater the mobile fluid saturation and mobile fluid porosity, while the mobile fluid saturation and physical properties in the Heshui area show a weak negative correlation, which is very different from the previous understanding. This further shows that physical property is not the main factor controlling the properties of movable fluid, and the difference of microscopic parameters will lead to the inconsistency between the properties of movable fluid and the traditional understanding.

*4.2. Effects on Moveable Fluid Parameters of Clay Minerals.* The correlation between clay minerals and movable fluid properties is relatively strong, indicating that compared with macroscopic characteristics, such as physical properties, microscopic characteristics have more significant effects on movable fluid properties (Figure 10). However, this trend is only applicable to the Jiyuan area, while the correlation in the Heshui area is poor, indicating that clay mineral characteristics are not the main controlling factor of movable fluid properties. In all kinds of clay minerals, illite, chlorite, I/S mixed layer, and movable fluid properties are basically negatively correlated. SEM results show that these minerals mainly exist in pores and hinder fluid movement. However, the consolidation capacity of kaolinite is relatively weak, and it can move with the fluid movement. The reservoir with kaolinite development generally represents that there are many feldspar dissolution pores, and the pores are relatively large, creating conditions for fluid movement.

*4.3. Effects on Moveable Fluid Parameters of Pore Structure Differences.* In general, the moveable fluid saturation of the two areas is both relatively low, while their saturation difference is as high as 7.71%. According to the analysis above, it is concluded that the most obvious difference between these two areas is the microscopic pore structure. Among the parameters representing characteristics of microscopic pore structure, throat radius, pore-throat radius ratio, and pore-throat amount allocation ratio are selected to analyze and to compare their effects on moveable fluid saturation due to the huge differences between the two areas (Figure 11). Figure 11 shows that throat radius and pore-throat amount allocation ratio are positively correlated to moveable fluid saturation, and the relativity is good with a relative coefficient of 0.5688 and 0.7158, respectively. Pore-throat radius ratio is negatively correlated to moveable fluid saturation with a relative coefficient of 0.8741 showing good relativity.

It is shown from the analysis above that those parameters representing the differences of microscopic pore structures, such as throat radius, pore-throat radius ratio, and pore-throat amount allocation ratio, are closely correlated to moveable fluid saturation in the reservoir. And from the analysis for the allocations of pore and throat radius in the two areas, it is concluded that the difference in throat radius and the amount of throat in a unit volume are the essential factors resulting in the difference in throat radius, pore-throat radius ratio, and pore-throat amount allocation ratio. The throat development degree in the Jiyuan area is much higher than that in the Heshui area, resulting in a poorer pore connectivity and a higher amount of ineffective pore in the Jiyuan area. And to some extent, this phenomenon leads to the difference in the moveable fluid saturation in the two areas. In other words, the difference in the throat development degree is the most significant factor resulting

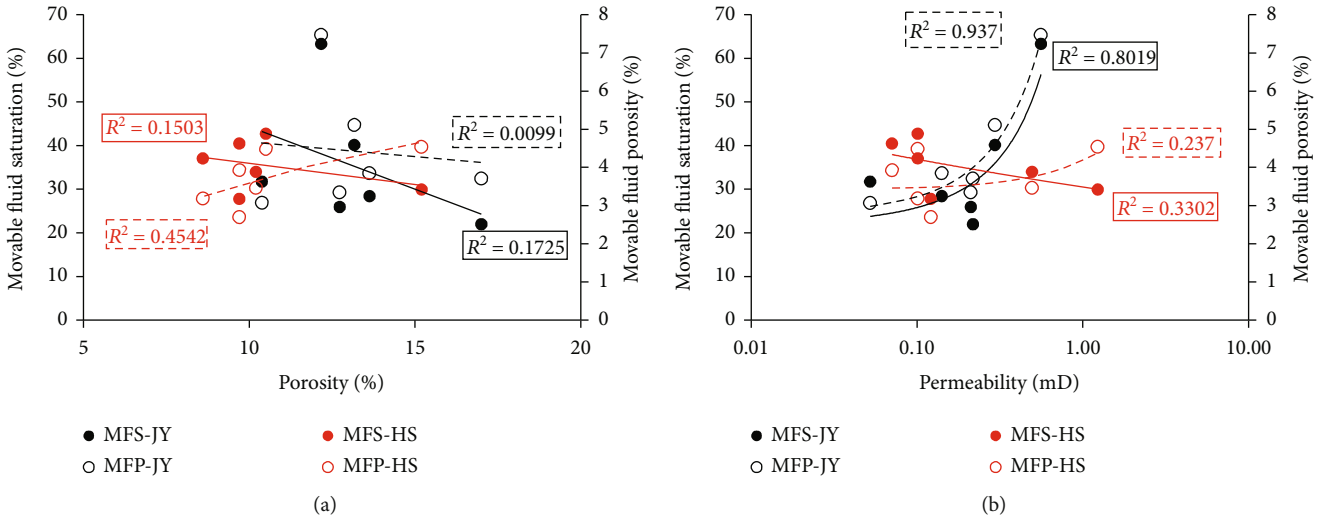


Figure 9: Relationship between physical properties and movable fluid parameters. MFS-JY: movable fluid saturation in Jiyuan; MFP-JY: movable fluid porosity in Jiyuan; MFS-HS: movable fluid saturation in Heshui; MFP-HS: movable fluid porosity in Heshui.

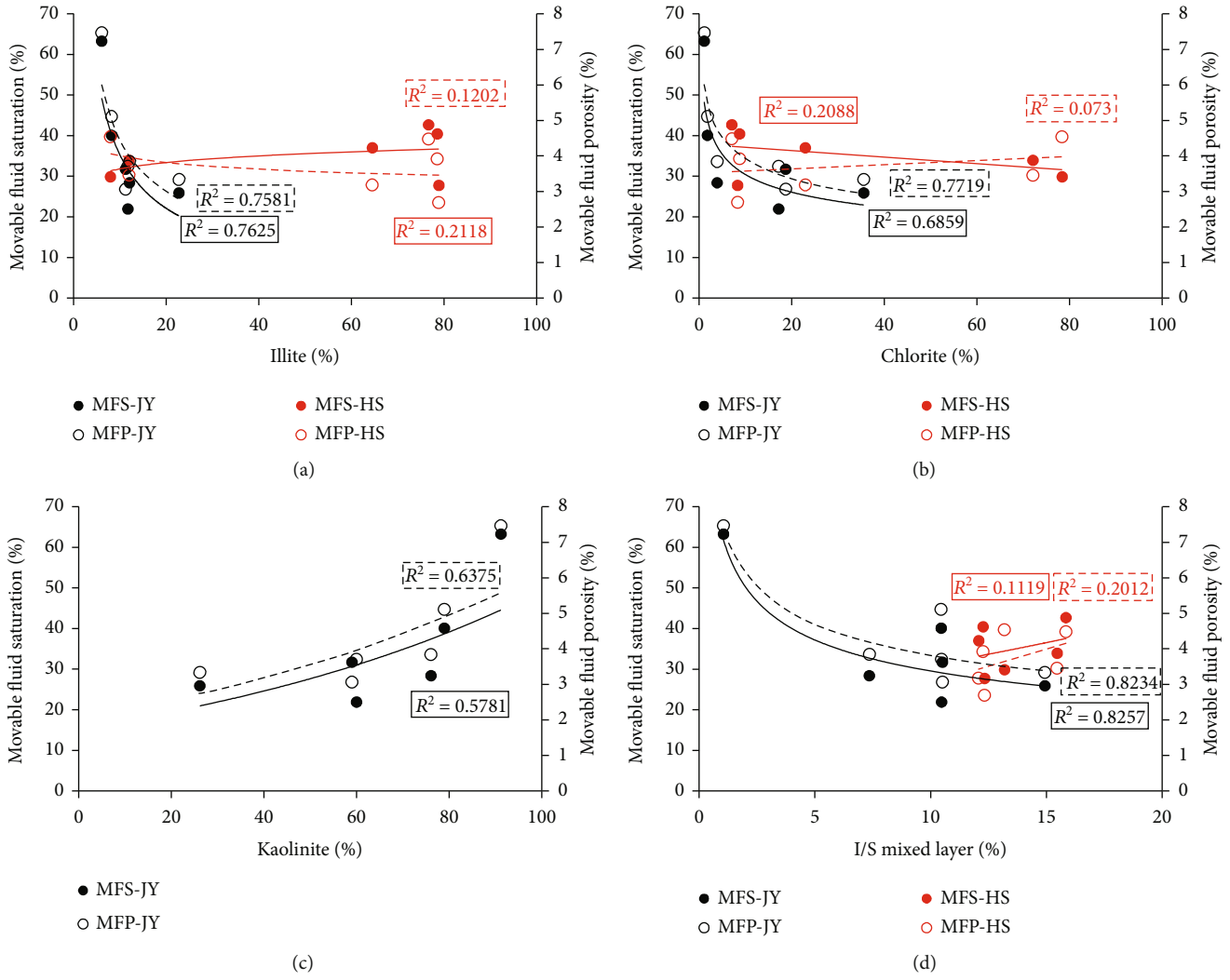


Figure 10: Relationship between clay mineral content and movable fluid parameters. MFS-JY: movable fluid saturation in Jiyuan; MFP-JY: movable fluid porosity in Jiyuan; MFS-HS: movable fluid saturation in Heshui; MFP-HS: movable fluid porosity in Heshui.

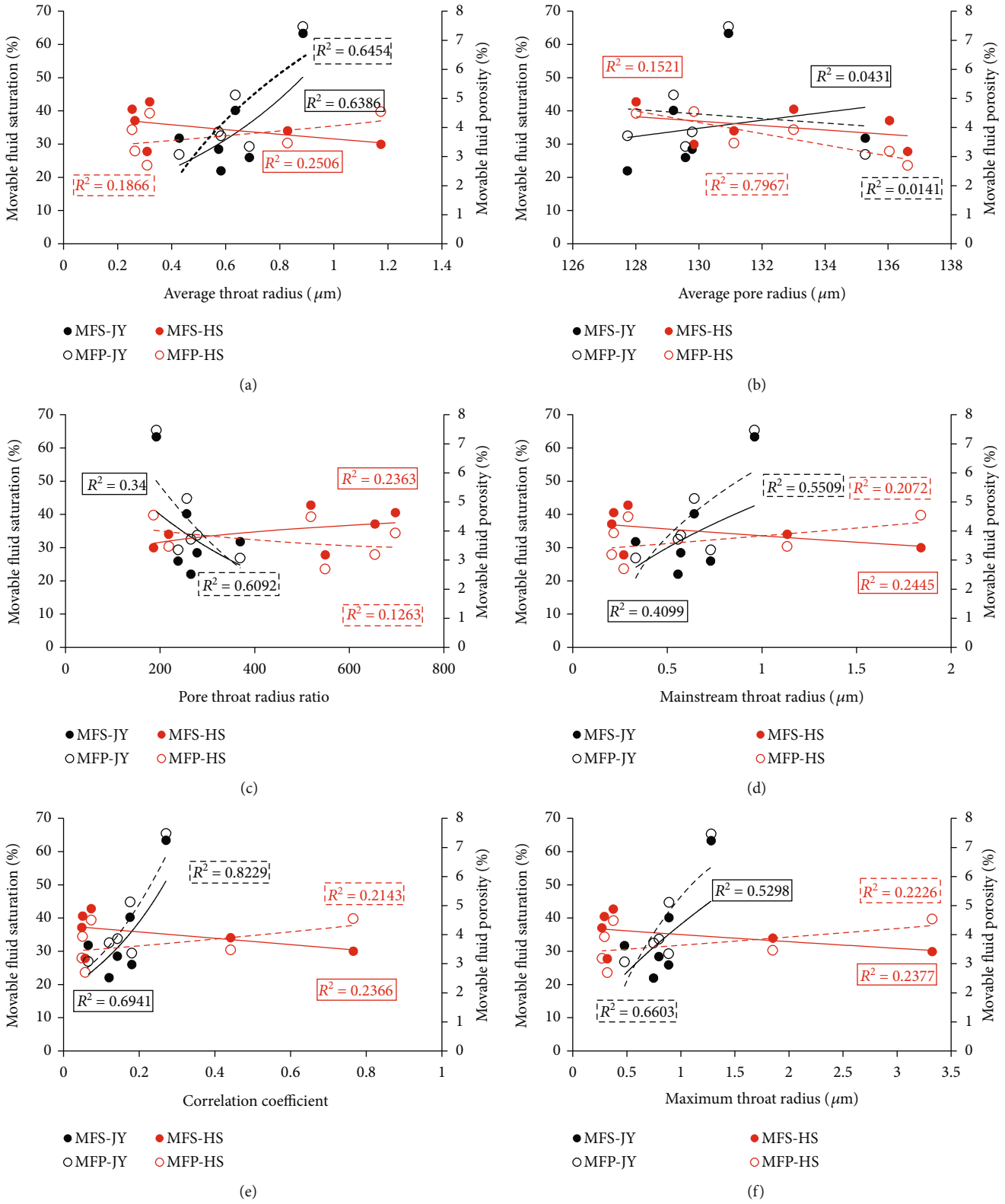


Figure 11: Relationship between pore structure-related properties and movable fluid parameters. MFS-JY: movable fluid saturation in Jiyuan; MFP-JY: movable fluid porosity in Jiyuan; MFS-HS: movable fluid saturation in Heshui; MFP-HS: movable fluid porosity in Heshui.

in the difference in moveable fluid saturation in the Heshui and Jiyuan areas.

## 5. Conclusions

Through analysis of petrologic, microscopic pore, moveable fluid saturation characteristics, and the relationship between the previous two parameters, the following conclusions can be made:

(1) In the Jiyuan area, sandstone type of Chang 6 member is mainly fine-ultra fine arkose, while in the Heshui area, it is mainly fine-ultra rock fragments-feldspar. Cementation types are mainly pore and enlarged-pore cementation. Interstitial materials are mainly kaolinite, illite, chlorite, and calcite. The differences in the relative amount of matrix in the two areas are huge, while pore types are almost the same. Pore combinations in both areas are mainly dissolution and intergranular pores

(2) There is a slight difference in the average pore radius. The main differences in their microscopic pore structures are the differences in the throat radius and the amount of throat. The average throat radius of the samples in the Jiyuan area is 0.61 $\mu$m while that in the Heshui area is 0.35 $\mu$m. The average pore-throat amount allocation ratio per unit volume in the Jiyuan area is 1.57 while that in the Heshui area is 1.32. Throat developed better in the Jiyuan area than that in the Heshui area

(3) As the parameters representing the differences of reservoir microscopic pore structure in the Jiyuan and the Heshui areas, throat radius, pore-throat radius ratio, and pore-throat amount allocation ratio correlate very well to the moveable fluid saturation. The difference in the microscopic pore structure of Chang 6 member between the two areas, especially the difference in their throat development degree results in the difference in moveable fluid saturation in the two areas

## Data Availability

The experimental data used to support the findings of this study are included within the manuscript and the supplementary materials.

## Conflicts of Interest

The authors declare that there are no conflicts of interest regarding the publication of this paper.

## Acknowledgments

The authors thank to my colleagues for their valuable advice. The research was supported by the Shaanxi Natural Science Basic Research Program, China (No. 2021JM-543) and the Research on Tight Gas Well Type Optimization and Improvement EUR Technology (No. 2021DJ2105).

## Supplementary Materials

The supplementary materials contained the data of CRMI and NMR. *(Supplementary Materials)*

## References

[1] J. Lai, G. Wang, Y. Ran, Z. Zhou, and Y. Cui, "Impact of diagenesis on the reservoir quality of tight oil sandstones: the case of upper Triassic Yanchang formation Chang 7 oil layers in Ordos Basin, China," *Journal of Petroleum Science and Engineering*, vol. 145, pp. 54–65, 2016.

[2] D. Ren, X. Wang, Z. Kou et al., "Feasibility evaluation of CO2 EOR and storage in tight oil reservoirs: a demonstration project in the Ordos basin," *Fuel*, vol. 331, article 125652, 2023.

[3] R. Freedman, S. Lo, M. Flaum, G. Hirasaki, A. Matteson, and A. Sezginer, "A new NMR method of fluid characterization in reservoir rocks: experimental confirmation and simulation results," *Spe Journal*, vol. 6, no. 4, pp. 452–464, 2001.

[4] D. Liu, D. Ren, K. Du, Y. Qi, and F. Ye, "Impacts of mineral composition and pore structure on spontaneous imbibition in tight sandstone," *Journal of Petroleum Science and Engineering*, vol. 201, article 108397, 2021.

[5] M. Wang, J. Xie, F. Guo, Y. Zhou, X. Yang, and Z. Meng, "Determination of NMR T2 cutoff and CT scanning for pore structure evaluation in mixed siliciclastic–carbonate rocks before and after acidification," *Energies*, vol. 13, no. 6, p. 1338, 2020.

[6] D. Ren, L. Ma, D. Liu, J. Tao, X. Liu, and R. Zhang, "Control mechanism and parameter simulation of oil-water properties on spontaneous imbibition efficiency of tight sandstone reservoir," *Frontiers in Physics*, vol. 10, p. 47, 2022.

[7] L. Jin, W. Guiwen, C. Min et al., "Pore structures evaluation of low permeability clastic reservoirs based on petrophysical facies: a case study on Chang 8 reservoir in the Jiyuan region, Ordos basin," *Petroleum Exploration and Development*, vol. 40, no. 5, pp. 606–614, 2013.

[8] J. Lai, G. Wang, Y. Chai, Y. Ran, and X. Zhang, "Depositional and diagenetic controls on pore structure of tight gas sandstone reservoirs: evidence from lower Cretaceous Bashijiqike formation in Kelasu Thrust Belts, Kuqa Depression in Tarim basin of West China," *Resource Geology*, vol. 65, no. 2, pp. 55–75, 2015.

[9] S. Huang, Y. Wu, X. Meng, L. Liu, and W. Ji, "Recent advances on microscopic pore characteristics of low permeability sandstone reservoirs," *Advances in Geo-Energy Research*, vol. 2, no. 2, pp. 122–134, 2018.

[10] D. Ren, H. Zhang, Z. Wang, B. Ge, D. Liu, and R. Zhang, "Experimental study on microscale simulation of oil accumulation in sandstone reservoir," *Frontiers in Physics*, vol. 10, 2022.

[11] U. Kuila and M. Prasad, "Specific surface area and pore-size distribution in clays and shales," *Geophysical Prospecting*, vol. 61, no. 2, pp. 341–362, 2013.

[12] A. J. Bolton, A. J. Maltman, and Q. Fisher, "Anisotropic permeability and bimodal pore-size distributions of fine-grained marine sediments," *Marine and Petroleum Geology*, vol. 17, no. 6, pp. 657–672, 2000.

[13] G. Weng, Q. Xie, C. Xu, P. Zhang, and X. Zhang, "Seismic response of cable-stayed spanning pipeline considering medium-pipeline fluid–solid coupling dynamic effect," *PRO*, vol. 11, no. 2, p. 313, 2023.

[14] Y. Xuanjun, L. Senhu, L. Qun et al., "Lacustrine fine-grained sedimentary features and organicrich shale distribution pattern: a case study of Chang 7 member of Triassic Yanchang formation in Ordos basin, NW China," *Petroleum Exploration and Development*, vol. 42, no. 1, pp. 37–47, 2015.

[15] D. Ren, D. Zhou, D. Liu, F. Dong, S. Ma, and H. Huang, "Formation mechanism of the upper Triassic Yanchang formation tight sandstone reservoir in Ordos basin-take Chang 6 reservoir in Jiyuan oil field as an example," *Journal of Petroleum Science and Engineering*, vol. 178, pp. 497–505, 2019.

[16] M. Baoquan, C. Shumin, Y. Weilin et al., "Pore structure evaluation of low permeability clastic reservoirs based on sedimentation diagenesis: a case study of the Chang 8 reservoirs in the Zhenbei region, Ordos basin," *Journal of Petroleum Science and Engineering*, vol. 196, article 107841, 2021.

[17] Y. Zhang, B. Ju, M. Zhang et al., "The effect of salt precipitation on the petrophysical properties and the adsorption capacity of shale matrix based on the porous structure reconstruction," *Fuel*, vol. 310, article 122287, 2022.

[18] G. Sheng, Y. Su, and W. Wang, "A new fractal approach for describing induced-fracture porosity/permeability/ compressibility in stimulated unconventional reservoirs," *Journal of Petroleum Science and Engineering*, vol. 179, pp. 855–866, 2019.

[19] C. R. Clarkson, M. Freeman, L. He et al., "Characterization of tight gas reservoir pore structure using USANS/SANS and gas adsorption analysis," *Fuel*, vol. 95, pp. 371–385, 2012.

[20] J. Lai, G. Wang, Z. Wang et al., "A review on pore structure characterization in tight sandstones," *Earth-Science Reviews*, vol. 177, pp. 436–457, 2018.

[21] C. R. Clarkson, N. Solano, R. M. Bustin et al., "Pore structure characterization of North American shale gas reservoirs using USANS/SANS, gas adsorption, and mercury intrusion," *Fuel*, vol. 103, pp. 606–616, 2013.

[22] F. Zhang, Z. Jiang, W. Sun et al., "A multiscale comprehensive study on pore structure of tight sandstone reservoir realized by nuclear magnetic resonance, high pressure mercury injection and constant-rate mercury injection penetration test," *Marine and Petroleum Geology*, vol. 109, pp. 208–222, 2019.

[23] H. Zhao, Z. Ning, Q. Wang et al., "Petrophysical characterization of tight oil reservoirs using pressure- controlled porosimetry combined with rate-controlled porosimetry," *Fuel*, vol. 154, pp. 233–242, 2015.